THERMAL STRUCTURES TECHNOLOGY DEVELOPMENT FOR REUSABLE LAUNCH VEHICLE CRYOGENIC PROPELLANT TANKS

Theodore F. Johnson
Roderick Natividad
H. Kevin Rivers
Russell Smith
MS 396
NASA, Langley Research Center
Hampton, VA 23681-0001
(757) 864-5418, 864-4204, 864-5428, and 864-3122

Abstract

Analytical and experimental studies conducted at the NASA Langley Research Center for investigating integrated cryogenic propellant tank systems for a Reusable Launch Vehicle are described. The cryogenic tanks are investigated as an integrated tank system. An integrated tank system includes the tank wall, cryogenic insulation, Thermal Protection System (TPS) attachment sub-structure, and TPS. Analysis codes are used to size the thicknesses of cryogenic insulation and TPS insulation for thermal loads, and to predict tank buckling strengths at various ring frame spacings. The unique test facilities developed for the testing of cryogenic tank components are described. Testing at cryogenic and high-temperatures verifies the integrity of materials, design concepts, manufacturing processes, and thermal/structural analyses. Test specimens ranging from the element level to the subcomponent level are subjected to projected vehicle operational mechanical loads and temperatures. The analytical and experimental studies described in this paper provide a portion of the basic information required for the development of light-weight reusable cryogenic propellant tanks.

INTRODUCTION

One of the goals for the next generation of launch vehicles is an order of magnitude reduction in the cost of delivering a payload to orbit. Recent studies on space transportation by the National Aeronautics and Space Administration (NASA) (Freeman, Stanley, Camarda, Lepsch, and Cook 1994) (NASA 1993) indicate that a Single-Stage-To-Orbit (SSTO) Reusable Launch Vehicle (RLV), fueled by Liquid Hydrogen (LH_2) and Liquid Oxygen (LOX) has the potential to reach this goal. The X-33/RLV Program is a partnership between NASA and industry to create a viable RLV (Baumgartner 1997). In this program, current and emerging technologies are utilized to develop and build the X-33, a 1/2 scale RLV demonstrator/test-bed vehicle (Cook 1996). These technologies are being pursued to develop an RLV that has efficient, and airline-like operation with 7-day refurbishment cycles between missions to reduce the operational costs, thereby reducing the cost to place a payload in orbit.

Large reusable cryogenic tanks will be required to contain the LH_2 and LOX for an SSTO RLV. The development and fabrication of reusable cryogenic tanks is one of the significant technical challenges to be overcome to develop an operable RLV (Cook 1996). Large expendable cryogenic tanks have been made for launch vehicles, but the durability of flight-weight reusable cryogenic propellant tanks has not been demonstrated. Cryogenic tank development is critical for an RLV because the tanks may comprise as much as 70 to 80 percent of the volume of the vehicle, as shown in figure 1 for two generic RLV's (Freeman, Stanley, Camarda, Lepsch, and Cook 1994). The cryogenic tanks of an RLV must not only function as pressure vessels at cryogenic temperatures, but they also must carry primary structural loads and support the Thermal Protection System (TPS). The cryogenic tanks, along with the TPS, must be easy to maintain, easy to repair, and reusable for the life of the vehicle.

In this paper, candidate reusable cryogenic propellant tank concepts are evaluated as a part of an integrated tank system that includes TPS, TPS attachment sub-structure, cryogenic insulation, and Integrated Vehicle Health

Monitoring (IVHM) (Melvin, Childers, Rogowski, ... 1997). Thermal and structural analyses are used to compare several candidate combinations of cryogenic tanks and TPS. Thermal-mechanical tests of cryogenic insulation, adhesives, structural elements, and subcomponents are performed, with the thermal and mechanical loading becoming increasingly complex as the specimen size increases. Test environments include: temperatures ranging from 20 K (-423˚F) to 810 K (1000˚F), pressures ranging from atmospheric to 372 kPa (54 psig), and mechanical loads of uniaxial tension, compression, and biaxial tension. This paper describes integrated cryogenic tank analysis, testing, and test facilities development at the NASA Langley Research Center (LaRC), which support technology development for a reusable LH_2 tank for an RLV.

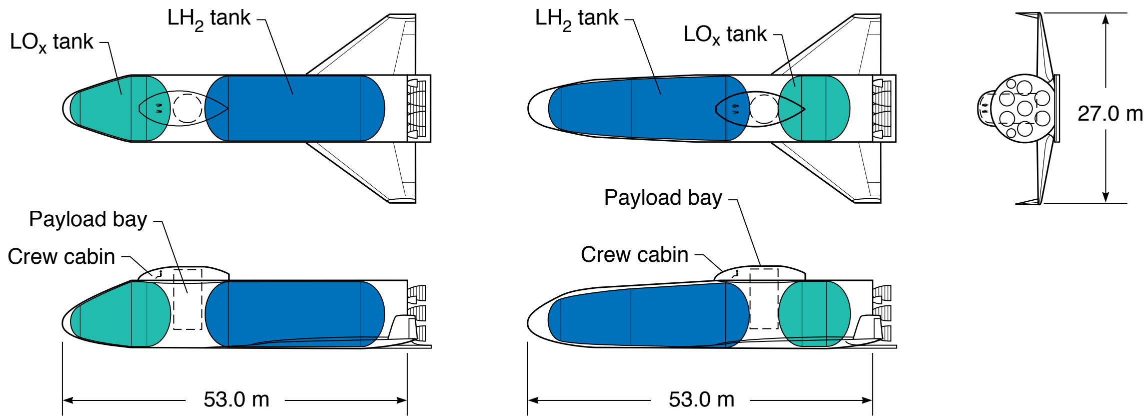

FIGURE 1. Reusable Launch Vehicle, NASA Langley Research Center Generic Vehicle (NASA 1993) with an Aft- or Forward-Located Liquid Hydrogen Tank.

ANALYTICAL STUDIES OF INTEGRATED CRYOGENIC SYSTEMS

The thermal and structural performance of the tank, cryogenic insulation, and TPS should be considered as a system to develop the best cryogenic tank for an RLV. Several combinations of LH_2 tank walls and TPS are analyzed to identify attractive concepts. An example of an integrated tank system design is displayed in figure 2. The titanium (Ti) sandwich wall acts as a pressure vessel, cryogenic insulation, primary structure, and TPS support. Extra Low Interstitial (ELI) titanium is used to reduce hydrogen embrittlement. The exterior facesheet does not have to be impermeable to LH_2 or LOX thus, mechanical fasteners can penetrate the external facesheet to attach TPS. Gaskets beneath the TPS panel gaps prevent subsurface hot gas flow during re-entry.

Integrated tank concepts considered in the analytical studies are depicted in figure 3 and listed in Table 1. The external foam concepts are based upon a forward-located, IM7/977-2 Graphite-Epoxy (Gr-Ep) ring and stringer stiffened tank concept from the X-33 Phase I Rockwell vehicle (Anonymous I 1995) that uses adhesively bonded Rohacell™ as the cryogenic foam insulation and either Alumina Enhanced Thermal Barrier (AETB) or Tailorable Advanced Blanket Insulation (TABI) as the TPS. Honeycomb cryogenic insulation concepts consist of a sandwich tank wall with an evacuated core for insulation and Superalloy/Honeycomb (SA/HC) metallic panels as TPS. Several material combinations are considered for the honeycomb sandwich tank wall. The Aluminum 2219-T87 aluminum sandwich tank concept (Al/Ti/Al) is considered because aluminum is compatible with LH_2 and the titanium core can either be brazed or adhesively bonded to the aluminum facesheet. The titanium honeycomb core provides sufficient insulation if evacuated and enhances the structural stability of the tank. The concept with titanium facesheets and titanium honeycomb core is investigated because of the high strength and operation temperature (645 K, 700˚F) of a brazed (Ti/Ti/Ti) concept. A concept consisting of IM7/5260 Graphite-Bismaleimide (Gr-BMI) facesheets with titanium honeycomb core is also considered because Gr-BMI has a moderately high operating temperature (450 K, 350˚F). In the final concept, Gr-BMI facesheets are combined with a Hexcel™ glass Reinforced Phenolic (HRP). The (Gr-BMI/HRP/Gr-BMI) concept has reduced thermal conductivity because of the non-metallic honeycomb core. Both Gr-BMI sandwich concepts can be adhesively bonded or co-cured sandwich structures. Thermal and structural analyses are used to compare the weights and strengths of these integrated tank systems. In the thermal analysis, the thicknesses of the cryogenic insulation and TPS insulation are sized to control the various operational temperatures. In the structural analysis, the structural stability of the tank wall is investigated for a given concept with various ring frame spacings.

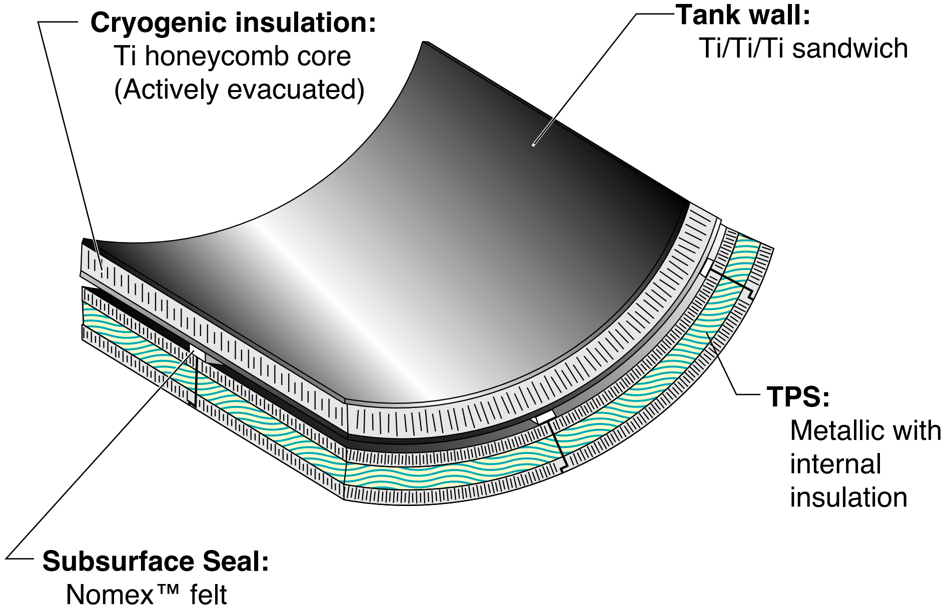

FIGURE 2. Example of an All Metallic (Titanium/Titanium/Titanium) Sandwich Cryogenic Tank with Metallic Thermal Protection System Integrated Tank System Concept for a Reusable Launch Vehicle.

TABLE 1. Honeycomb Sandwich Cryogenic Tank Walls.

FACESHEET/CORE/FACESHEET	ABBREVIATION
Aluminum/Titanium/Aluminum	(Al/Ti/Al)
Titanium/Titanium/Titanium	(Ti/Ti/Ti)
Graphite-Bismaleimide/Titanium/Graphite-Bismaleimide	(Gr-BMI/Ti/Gr-BMI)
Graphite-Bismaleimide/Hexcel™ glass Reinforced Phenolic/Graphite-Bismaleimide	(Gr-BMI/HRP/Gr-BMI)

Thermal Sizing Study

A thermal sizing study of the designs in figure 3 was conducted to compare the thermal performance of each cryogenic tank concept. The cryogenic insulation thicknesses and TPS were sized to maintain temperatures within the limits shown in fig. 3 using a one-dimensional finite element sizing code (Myers 1998). The weight of the resulting TPS and cryogenic insulation (honeycomb core for sandwich tank walls) was calculated and compared for each tank/TPS system. The thermal mass of the tank wall membrane (sized to withstand the pressurization load and to limit LH_2 permeation in the case of composite walls) was included in the thermal sizing analysis. The criteria used for sizing the thickness of the cryogenic insulation and TPS were: a constant temperature of 20 K (-423˚F) at the tank wall, prevention of frost build-up and air liquefaction on the tank's cryogenic insulation surface during ground-hold, and limiting the maximum operational temperatures (shown in figure 3) of the various materials used in the vehicle's structure and TPS during re-entry. All of the sandwich tanks had a lower limit temperature of 115 K (-250˚F) on the outer facesheet during ground-hold to minimize air liquefaction. The windward side heating load was provided by Kay Wurster the Vehicle Analysis Branch (VAB) at LaRC for the vehicles in figure 1. These cylindrical study vehicles were used because the vehicles did not have cavities over the cryogenic tanks or an aeroshell, thus the tank wall-insulation-TPS was layered as in figure 2.

The mass of the cryogenic insulation and TPS are plotted in figure 4 versus the x-location along the length of the windward centerline of the vehicle. Although the LH_2 tank does not extend the entire length of the vehicle, the tank may be located either forward or aft as shown in figure 1. An all metallic concept, (Ti/Ti/Ti) with metallic TPS, is lighter than the other organic/ceramic or metallic concepts. The all metallic titanium concept is lighter because the relatively high use temperature of titanium requires less TPS for re-entry heating and the evacuated titanium honeycomb core acts as an effective insulator, eliminating the need for cryogenic insulation. The (Gr-BMI/HRP/Gr-BMI) concept's non-metallic core has reduced thermal conductivity and increased insulative capacity making this concept lighter than the other sandwich concepts except for the all titanium concept. The (Gr-BMI/HRP/Gr-BMI) concept is also lighter than the stiffened Gr-Ep concepts because the outer facesheet can be allowed to cool to a temperature of 115 K (-250˚F) during ground-hold. The upper use temperature limit and low heat capacity of the Rohacell™ (480 K, 400˚F) external cryogenic foam increases the TPS thickness for the stiffened Gr-Ep structure making the concept heavier than the all titanium concept. The (Al/Ti/Al) and (Gr-BMI/Ti/Gr-BMI) tanks are the heaviest concepts. These two concepts do not effectively use the higher temperature capability of the titanium core because of their facesheets' lower maximum operating temperature during re-entry. The aluminum concept is not included in the structural buckling study.

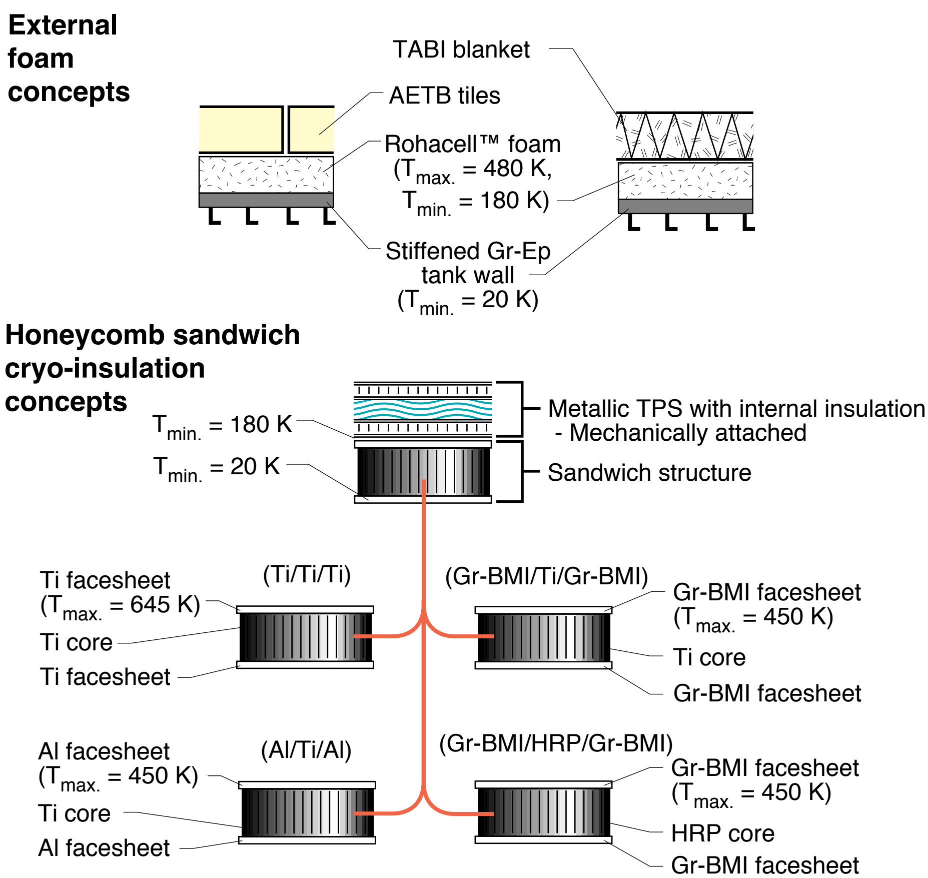

FIGURE 3. Concepts Used in the Thermal Sizing and Structural Buckling Studies.

Structural Buckling Study

A structural buckling study is performed with the more attractive tank concepts identified in the thermal sizing study. The weight of the tank's structural elements and the effects of varying ring frame spacing on tank stability are compared in the structural buckling study. This structural study focuses on determining the buckling strength of an unpressurized LH_2 tank during the ground-hold and soak-through phase of a vehicle mission-profile. Pressure stabilization is ignored so that the tank is designed with sufficient strength to support a full LOX tank in the event of tank depressurization. A non-linear shell of revolution code, BOSOR4 (Bushnell 1977), is used in the study. A representative model of a sandwich tank wall structure and the boundary conditions used in the analysis are shown in figure 5. The model has periodic boundary conditions simulating an infinitely long cylindrical tank. The ring frame design is kept fixed in this study to reduce the number of variables, but the ring frame spacing is varied for all of the models. The core thicknesses from the thermal sizing study are also used in the buckling models.

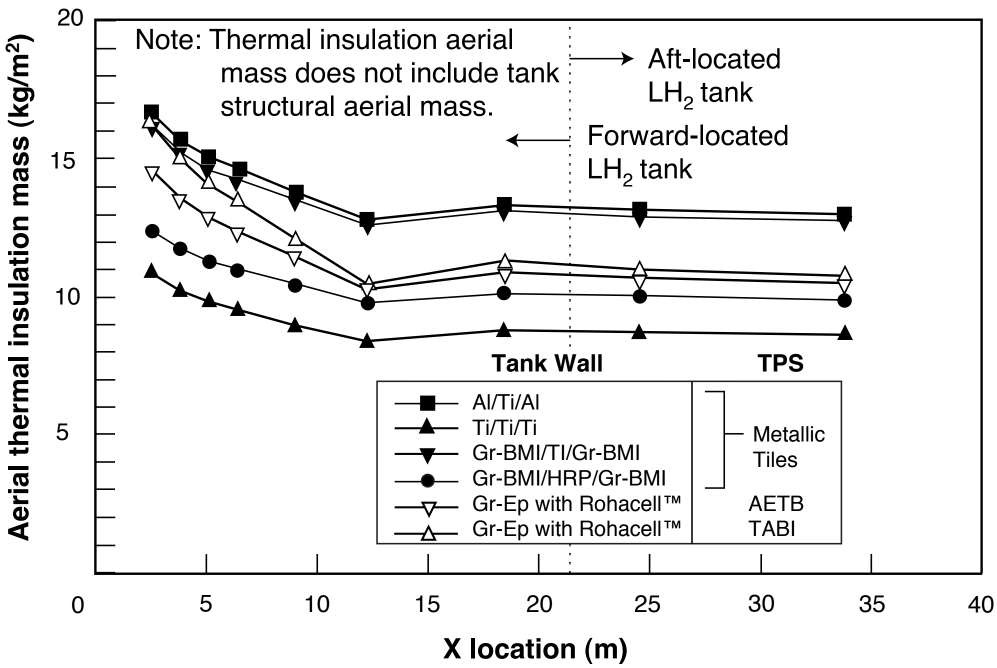

FIGURE 4. Aerial Masses of TPS and Cryogenic Insulation Along the Generic Vehicle's Windward Centerline for a Liquid Hydrogen Tank.

Boundary Conditions

Left End		Right End	
Pre-Buckling	Buckling	Pre-Buckling	Buckling
u - free v - free w - free $w_{,x}$ - fixed	u - fixed v - free w - free $w_{,x}$ - fixed	u - fixed v - free w - free $w_{,x}$ - fixed	u - fixed v - free w - free $w_{,x}$ - fixed

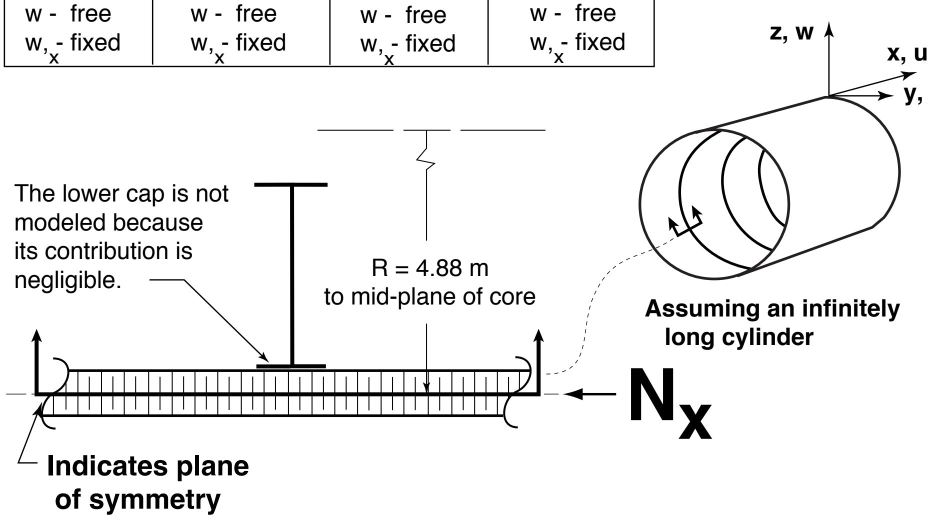

FIGURE 5. The Boundary Conditions, Model Orientation, and Model Used in BOSOR4 for the Structural Buckling Study.

The concepts evaluated in the structural buckling study are (Ti/Ti/Ti), (Gr-BMI/HRP/Gr-BMI), and (Gr-BMI/Ti/Gr-BMI) sandwich concepts, and Gr-Ep ring and stringer stiffened tank concepts. The structural weight of the tank (not including the sandwich core material, cryogenic insulation or TPS), and the buckling strength of the tank are plotted using the ring frame spacing as the abscissa in figure 6. The (Gr-BMI/HRP/Gr-BMI) concept was found to have the same buckling response and weight as the (Gr-BMI/Ti/Gr-BMI) concept so it is not shown separately in figure 6. The curve in figure 6 for the (Ti/Ti/Ti) concept shows a reduction in buckling strength for a ring frame spacing less than 1.5 m (60 in.) because the buckling mode changes from panel buckling to local buckling in the ring frame. The (Ti/Ti/Ti) tank concept fails in a collapse mode at a low ring frame spacing, placing a high compression load in the ring frame. The other tank concepts all buckle between ring frames in a panel failure mode.

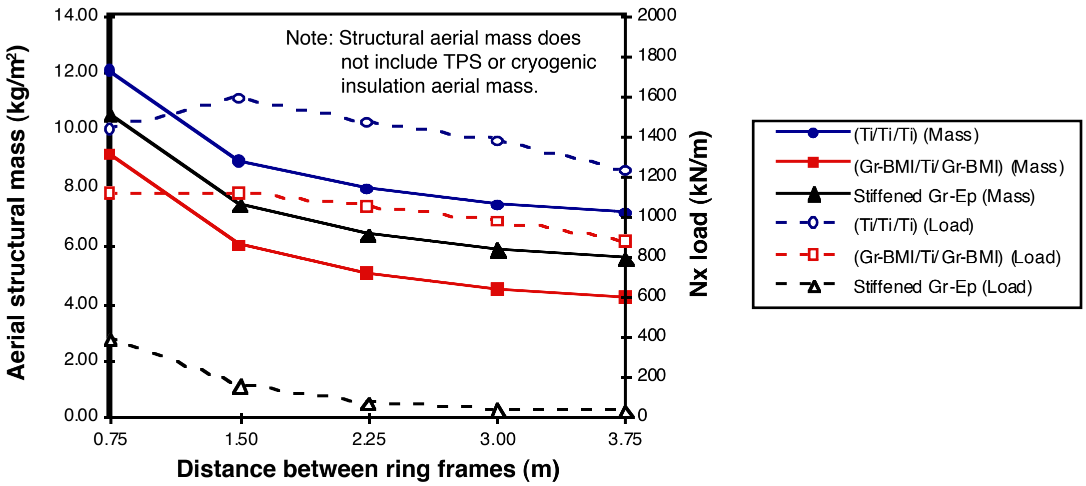

FIGURE 6. Structural Buckling Study Aerial Masses and Critical Buckling Loads for Sandwich Skin Tanks and a Forward-Located Graphite-Epoxy Ring and Stringer Stiffened Tank.

An aft-located LH_2 tank which does not rely on pressure stabilization must be able to resist a minimum buckling load of 630 kN/m (3.6 kips/in.) due to the weight of a forward-located LOX tank and a payload during launch. A vehicle with a forward-located LH_2 tank does not experience the maximum axial compression load until after landing. The buckling load in this case is 300 kN/m (1.720 kips/in.) due to bending (Anonymous II 1995) when the vehicle is horizontal after landing in an unpressurized state. All of the sandwich tank concepts buckle well above all load requirements at all ring frame spacings studied. The Gr-Ep ring and stringer stiffened tank is designed as a forward-located LH_2 tank and requires a 0.75 m (30 in.) ring frame spacing to resist a 300 kN/m (1.720 kips/in.) buckling load. The (Ti/Ti/Ti) tank at ring frame spacings greater than 1.5 m (60 in.) and a (Gr-BMI/Ti/Gr-BMI) tank at all ring frame spacings is lighter than a Gr-Ep ring and stiffened structure at a 0.75 m (30 in.) spacing. An aft-located, non-pressure-stabilized, Gr-Ep ring and stringer stiffened tank would weigh substantially more than the honeycomb tanks because of the additional structural mass required to resist buckling and inertial loads due to the weight of a forward-located LOX tank and the payload. Thus, the results shown in figure 6 suggest that sandwich structures have a structural and weight advantage over stiffened Gr-Ep tanks.

Combined TPS, cryogenic insulation, and tank structural aerial masses are ranked by their total weight in Table 2. The studies demonstrate the advantages of sandwich structure in an integrated tank system design. Several sandwich tanks with metallic TPS and ring frame spacings of 3.0 m (120 in.) are lighter than the stiffened forward-located Gr-Ep concepts with ceramic TPS with a ring frame spacing of 0.75 m (30 in.). Sandwich tanks with larger ring frame spacings are not considered because of potential fabrication issues and increased pressure pillowing. The lightest tank concept is the (Gr-BMI/HRP/Gr-BMI) concept with metallic TPS. An all metallic (Ti/Ti/Ti) tank concept is the second lightest. Both concepts are not only lighter, but also have much higher buckling strengths than the Gr-Ep stiffened tank and have a weight advantage over Gr-Ep due to their higher operating temperatures. If the stiffened Gr-Ep forward-located tank is moved to an aft location, the structural mass of the tank would increase. These studies indicate that a honeycomb sandwich tank with mechanically attached metallic TPS is an attractive LH_2 tank system for an RLV. However, more detailed studies are required to corroborate the results from the analytical studies and any of the concepts studied will require verification of their insulative capacities, strengths, reliability, and durability through thermal, and structural testing.

TABLE 2. Combined Aerial Masses from the Thermal Sizing and Structural Buckling Studies with Variable Ring Frame Spacing.

TANK/TPS	RING FRAME SPACING (m)	CRYOGENIC INSULATION & TPS AERIAL MASS (kg/m^2)	TANK STRUCTURAL AERIAL MASS (kg/m^2)	TOTAL AERIAL MASS (kg/m^2)
(Gr-BMI/HRP/Gr-BMI)/(SA/HC)	3.0	10	6.0	16.0
(Ti/Ti/Ti)/(SA/HC)	3.0	8.9	8.9	17.8
(Gr-BMI/Ti/Gr-BMI)/(SA/HC)	3.0	12.8	6.0	18.8
Stiffened Gr-Ep/AETB	0.75	11.3	10.4	21.7
Stiffened Gr-Ep/TABI	0.75	11.7	10.4	22.1

TEST PROGRAM

A series of tests and test facilities have been developed during Phase I and Phase II of the X-33/RLV Program to further evaluate potential reusable cryogenic tank designs for RLV's. These tests provide information to verify the performance of a concept, to validate analysis methods, and to demonstrate the scalability of a tank design. The specimens vary in size from small elements to large subcomponents. The element and panel testing are performed to investigate specific aspects of the integrated tank design such as bonding methods, evacuation processes, cryogenic insulation integrity, and load carrying capability. Evaluating tank performance as an integrated tank system (tank structure, cryogenic insulation, and TPS) at operational temperatures and load conditions is critical to validate a design. Therefore, subcomponent testing of full-scale cryogenic tank sections under cyclic thermal and mechanical loading is performed to investigate additional thermal-structural interactions of the tank design and to validate performance and fabrication techniques. The cryogenic tank shown in figure 7, illustrates the uniaxial tension and compression panel tests, the cryogenic pressure box subcomponent test, and the mechanical loading each test is designed to simulate. Each of the tests requires the development of new, unique testing facilities and test procedures.

FIGURE 7. Cryogenic Tank Load Conditions Simulated in the Panel and Subcomponent Tests.

Element Tests

Element tests were developed to investigate specific design features under simplified load conditions to provide data that can be incorporated into the design of larger specimens. Two types of element tests are performed, the flatwise tension test and the sandwich core evacuation test or ravioli tests. In these tests, element specimens are cycled between temperatures of 20 K (-423˚F) and 395 K (250˚F). Flatwise tension tests investigate adhesive strengths after thermal cycling and sandwich evacuation tests investigate the feasibility of maintaining an evacuated core in a sandwich cryogenic tank wall.

Flatwise Tension Test

Adhesives are used to bond honeycomb core to composite facesheets and to bond cryogenic foam insulation to the tank wall. Flatwise tension tests (Glass 1997) are used to investigate the effects of cryogenic and elevated temperatures on the bond line pull-off strengths for sandwich tank walls and tank walls with adhesively bonded cryogenic insulation. Examples of flatwise tension specimens are shown in figure 8. When an adhesive is subjected to large changes in temperature, the adhesive may experience a phase transition, becoming brittle at low temperatures, and could be subject to stress relaxation or creep at elevated temperatures. A structural system subjected to large changes in temperature, may also develop high stresses induced by coefficient of thermal expansion mismatch resulting in debonding or core cracking without any mechanical load applied.

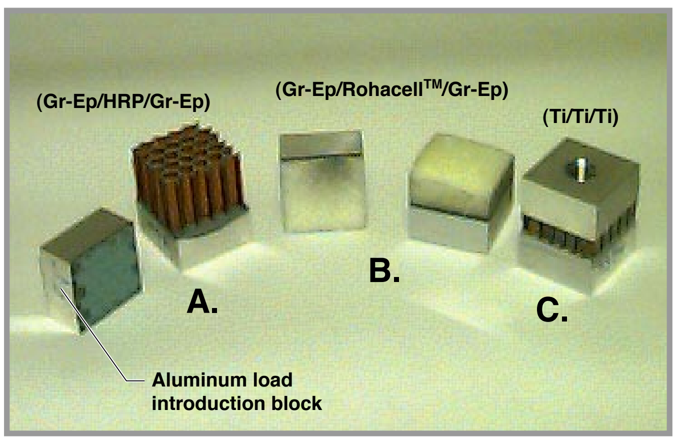

FIGURE 8. Flatwise Tension Specimens: A. Graphite-Epoxy/HRP/Graphite-Epoxy, B. Graphite-Epoxy/Rohacell™ /Graphite-Epoxy, C. Titanium/Titanium/Titanium.

The adhesive and facesheet/core combinations tested to date are listed in Table 3. Various types of adhesively bonded or co-cured 0.05 m x 0.05 m (2 in. x 2 in.) specimens are cycled from room temperature to cryogenic or elevated temperatures. Each specimen is then loaded to failure in tension at room temperature. In figure 9, the ultimate stress results are displayed for HRP honeycomb bonded to Gr-Ep facesheets as an example of the type of information generated from the flatwise tension tests. The room-temperature specimens are control specimens which are not thermally cycled, providing a baseline strength for a specimen type. Full details of the flatwise tension tests results are reported by Glass (Glass 1997). The remaining specimens were either thermally cycled from room temperature to 20 K (-423˚F) 10 times or from room temperature to 395 K (250˚F) 10 times.

The three best performing adhesives are EA 9394, Crest 3170, and HT 435. The EA 9394 is a room-temperature-cured adhesive and is widely used as a cryogenic adhesive. The Crest 3170 is also a room-temperature-cured adhesive and is stronger than EA 9394 after thermal cycling. The HT 435 is a high-temperature-cured adhesive (450 K, 350˚F) and has the best overall performance after being thermally cycled, however, this adhesive is the most sensitive to preparation procedures. The FM 300, a high-temperature-cured film adhesive (450 K, 350˚F) has the lowest strength and the PR 1664, a room-temperature-cured adhesive, also has a relatively low strength.

TABLE 3. Adhesives, Facesheets, and Core Materials Used in the Flatwise Tension Tests.

ADHESIVE **FACESHEET/ CORE**	**EA 9394**	**PR 1664**	**CREST 3170**	**FM 300**	**HT 435**	**CO-CURE**
Gr-Ep/						
Ti		√	√		√	
HRP	√	√	√	√	√	
Rohacell™ WF-71	√	√		√	√	
Nomex™	√	√		√		
Gr-BMI/						
Ti		√	√		√	
HRP						√
Nomex™	√			√	√	
Rohacell™ WF-71	√			√	√	
Al/						
Ti	√	√	√		√	
Stainless Steel/						
Rohacell™ WF-71	√	√	√			

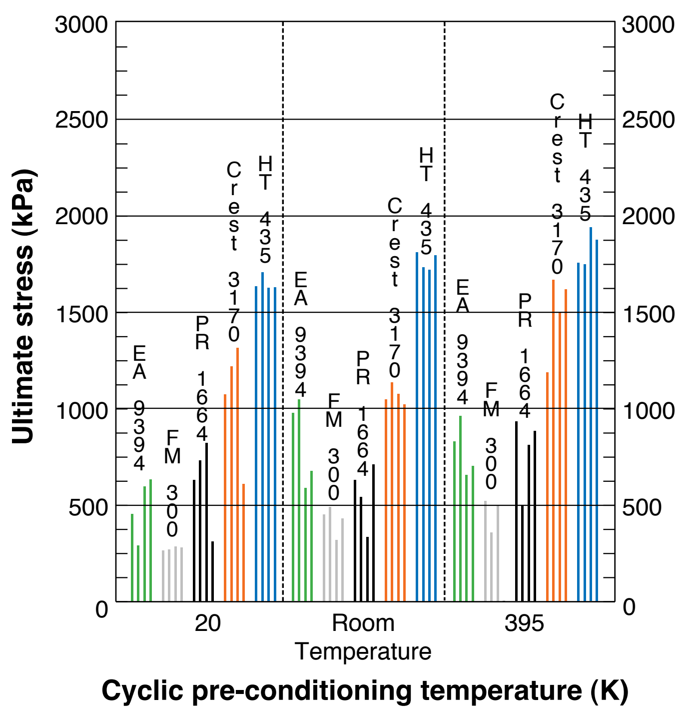

FIGURE 9. Flatwise Tension Strengths (Tested at Room Temperature) of HRP Honeycomb Core Bonded to Graphite-Epoxy with Five Different Adhesives and Having Three Different Pre-conditionings (Glass 1997). Each Bar Represents a Different Specimen Tested to Failure.

Sandwich Core Evacuation (Ravioli) Test

The core of a cryogenic sandwich tank may not only perform its structural function, but if evacuated, may also act as cryogenic insulation. Evacuating the core enhances its insulation capacity by reducing the thermal effects of natural convection and gas conduction and may eliminate the need for additional cryogenic insulation. It is essential to maintain a vacuum in the core to prevent cryopumping and potential failure of the sandwich.

A test was developed to evaluate the ability of various concepts for a sandwich tank wall system to resist gas permeation (Glass 1997). A series of evacuated core honeycomb specimens (figure 10) were fabricated and tested. The specimens were referred to as ravioli specimens due to their shape. A square of cryogenic foam insulation or perforated honeycomb core material with beveled edges is sealed inside of a 0.15 m x 0.15 m (6 in. x 6 in.) shell of Gr-Ep or Gr-BMI. The specimen is sealed by either bonding the two pre-cured halves with an adhesive or by co-curing the shell material around the core. The core material in these specimens is perforated or drilled to allow for evacuation due to air liquefaction/solidification from cryogenic temperatures or by mechanical evacuation. An evacuation stem (location shown in figure 10) is used to actively evacuate the specimen and allow any trapped gasses to escape as the specimen is warmed.

FIGURE 10. A Graphite-Epoxy and HRP Honeycomb Core Ravioli Specimen's Components and Top View of Assembled Specimen (Evacuation Stem Removed).

All six ravioli specimens tested are listed in table 4. Specimen 1 had a Rohacell™ core, but did not have an evacuation stem. This specimen was cycled from room temperature to 80 K (-320˚F) 10 times by immersing the specimen in a container filled with LN_2, removing the specimen, then allowing the specimen to warm to room temperature. There were no visible signs of damage. The specimen was also immersed once in liquid helium (LHe) and then removed. The specimen ruptured as it warmed to room temperature. It is believed that the specimen absorbed LHe into the core region and burst because the LHe vaporized faster than the gaseous helium (GHe) could out-gas. Each specimen listed in Table 4, except for specimen 1, had an evacuation stem attached on the upper portion of the specimen to actively evacuate the specimen and to allow the specimen to out-gas if LHe permeated to the core region. The specimens were thermally cycled 10 times to LN_2 temperatures (80 K, -320˚F), then immersed 2 times in LHe (4K, -450˚F) with no visible signs of degradation. The integrity of each specimen was then investigated after thermal cycling by evacuating the specimen as the specimen's temperature was lowered from ambient to 80 K (-320˚F). At various temperatures GHe was sprayed at the specimen's edges while a helium (He) mass spectrometer leak detector was used to actively evacuate the specimen and detect the amount of leakage of GHe into the specimen. The data from two leak detection tests for specimen 6 are shown in figure 11. The plot shows that as the specimen was cooled, the specimen's ability to maintain a low pressure diminished. The leaks in specimens 2 through 5 were too large for the He mass spectrometer leak detector to evacuate the specimen.

The results from the ravioli tests demonstrated that maintaining vacuum in even a small specimen is difficult, and as the specimen was cooled, its resistance to GHe permeation was reduced. The helium mass spectrometer leak detector could not localize the origin of GHe permeation. The GHe permeation into the specimens may have resulted from a coefficient of thermal expansion mismatch between the adhesive and the two shells causing microcracks in the bond line. A crease located on the top of the shell at the corners, as indicated in figure 10, may have also been a source of leakage. The co-cured specimen without an adhesive layer at the bond line performed only slightly better than the adhesively bonded specimens. These results suggest that improvements are needed in the fabrication of leak-free sandwich structures, and that a vented or an actively evacuated system may be required in an evacuated core sandwich structure.

TABLE 4. Graphite-Epoxy Ravioli Specimens.

SPECIMEN NO.	CORE MATERIAL	ADHESIVE	RESULT
1 (No evacuation stem)	Rohacell™ WF-110	FM 300	Rupture
2	Rohacell™ WF-51	FM 300	Large leaks
3	Rohacell™ WF-71	PR 1664	Large leaks
4	Nomex™ honeycomb	Crest 3170	Large leaks
5	Rohacell™ WF-110	Co-Cured	Large leaks
6	HRP honeycomb	EA 9394	Moderate vacuum held

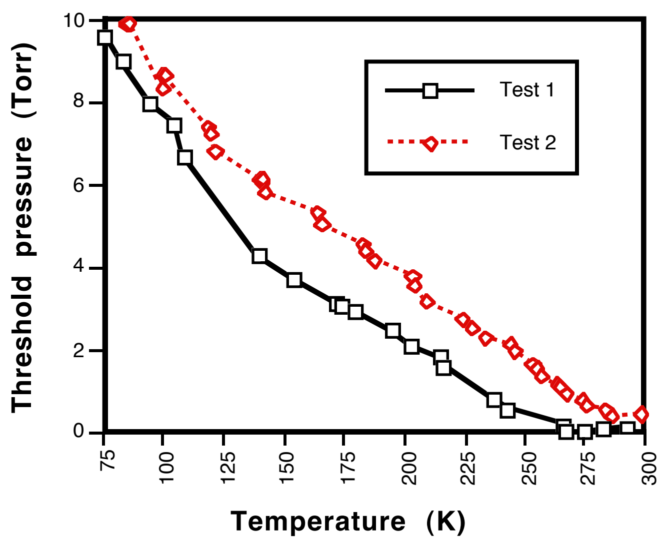

FIGURE 11. Pressure Versus Temperature for the 6th Ravioli Specimen (Glass 1997).

Panel Tests

Panel tests are being used to address integration issues between the tank wall and cryogenic insulation subjected to representative operational thermal and mechanical loads. The panel test specimens are larger than the element specimens and incorporate "lessons learned" from the element tests. Two types of panel tests are described: a cyclic uniaxial tension test to simulate hoop pressurization, and a static compression test to simulate structural and inertial loads, as depicted in figure 7. Only cryogenic insulation is integrated into the specimen for the panel tests to reduce the complexity of testing. Testing with TPS attached to the specimen would require additional heating equipment and would result in longer, more complicated testing cycles, and more expensive, elaborate test specimens.

Uniaxial Tension Tests

Combined cyclic thermal and mechanical tests of various cryogenic tank wall concepts were performed on flat 0.30 m x 0.60 m (1 ft x 2 ft) panel specimens. A flat specimen closely approximates a tank wall due to the tank's large radius. These tests were developed from earlier tests of a cryogenic insulation tile developed for the Advanced Launch System (ALS) (McAuliffe, Davis, and Taylor 1986). The purpose of the tests was to simulate both the thermal and mechanical loads experienced in an RLV mission from launch, to orbit, to re-entry. The cryogenic tanks in an RLV must endure biaxial tension loads associated with internal pressurization as well as maximum thermal and mechanical flight loads. However, for these tests the only mechanical load applied was a uniaxial tension load simulating circumferential pressure loading. These combined, cyclic, thermal-mechanical tests verify: the durability of the cryogenic insulation when subjected to cyclic mission-profile conditions, the bond line integrity between cryogenic insulation and the structure, the performance of cryogenic tank fabrication technologies at a small scale, and the effectiveness of various integrated health monitoring (IVHM) techniques.

Specialized test fixtures have been developed that allow a test specimen to be thermally cycled according to pre-defined temperature profiles between a minimum temperature of 20 K (-423˚F) and a maximum temperature of 645 K (700˚F). Figure 12 shows a typical specimen mounted in the fixture with the cryogenic chambers mounted on the surface of the inner tank wall of the specimen and a convective heating chamber adjacent to the external surface of the foam insulation. Tension load and temperatures for the cryogenic and high temperature chambers are independently controlled in a test cycle. A typical cycle lasts 30 to 80 minutes. An example of a thermal-mechanical load profile for a LH_2 tank specimen is shown in figure 13, which displays the complex tension loading and temperature profiles on the hot side and cryogenic side of the panel over a period of time.

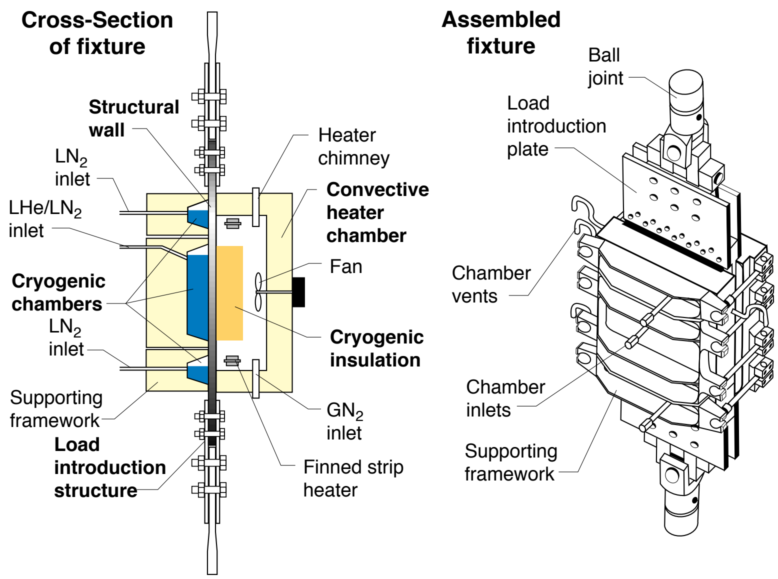

FIGURE 12. Schematic and Assembled View of the Test Fixture for the Uniaxial Tension Test.

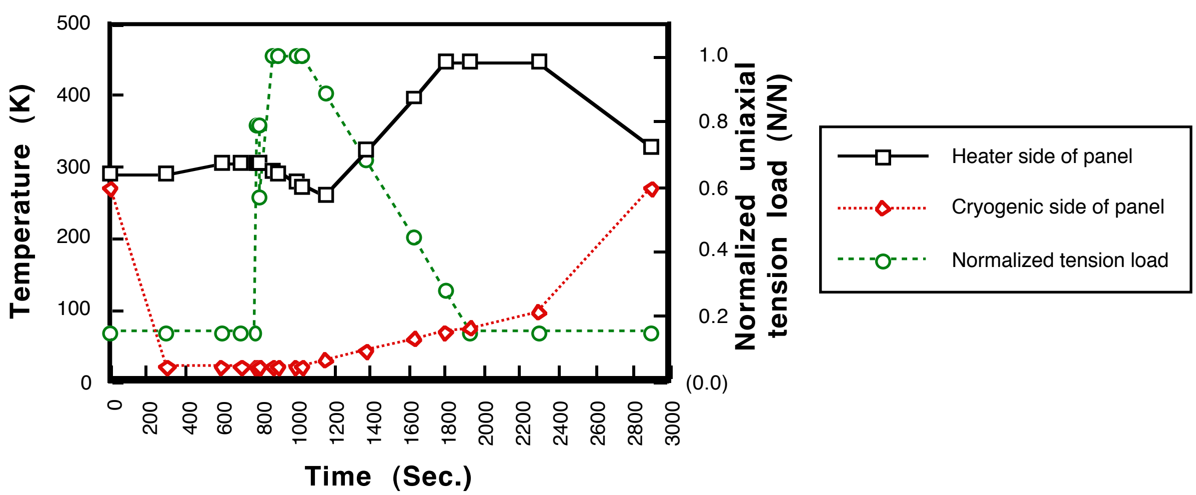

FIGURE 13. Typical Thermal-Mechanical Cycle for a Liquid Hydrogen Tank Specimen in the Uniaxial Tension Test.

All of the panels tested to date as a part of the X-33 Program Phase I and II are listed in Tables 5 and 6. Fiber-optic or IVHM thermal sensors were used on some of the panels tested (as indicated in Table 5). A meter of fiber-optic cable was coiled at several locations to obtain a point-wise thermal reading (Melvin, Childers, Rogowski, … 1997). A single fiber was used to monitor several locations on a specimen. The adhesive methods and the ability of the fiber optic thermal sensors to operate during mission profile conditions were tested in the uniaxial tension tests. The tests of panels LO-3 and LO-4 support qualification of the SS-1171 spray-on-foam insulation (SOFI) for the X-33's Al LOX tank, and future tests will support certifying Airex™ foam panels for the X-33's LH_2 tank domes.

TABLE 5. Experimental Results for the LOX Tank Concepts Tested.

LOX TANK PANEL	PANEL DESCRIPTION	NO. OF MISSION-PROFILES	RESULTS
LO-1	Al-Li* panel, EA 9394 adhesive, External Airex™ foam insulation	23	No cracks in foam. No disbonds.
LO-2	Al panel, EA 9394 adhesive, external Airex™ foam insulation	33	No cracks in foam. No disbonds.
LO-3	Al panel, external SS-1171, and PDL-1034 foam insulation	50	PDL-1034 cracked after 16 cycles. Insulation thickness reduced due to surface charring (no degradation in performance noticed).
LO-4	Al-Li* panel, external SS-1171 foam insulation, fiber-optics	50	No cracks in foam. Insulation thickness reduced due to surface charring (no degradation in performance noticed).

* Al-Li - Aluminum Lithium 2195

TABLE 6. Experimental Results for LH_2 Tank Concepts Tested.

LH_2 TANK PANEL	PANEL DESCRIPTION	NO. OF MISSION-PROFILES	RESULTS
LH-1	Gr-Ep panel, EA 9394 adhesive, external Airex™ foam insulation	42	Airex™ foam cracked after 42 cycles (due to a void in the adhesive layer).
LH-2	K3B/Ti/K3B† co-cured sandwich panel	12	Panel failed in the load introduction region after 12 cycles.
LH-3	K3B/Ti/K3B† co-cured sandwich panel with a joint	0	Panel failed in the joint region at 80% of the design limit load during a pre-test load check.
LH-4	Gr-Ep/Rohacell™ WF-71/Gr-Ep foam sandwich panel	25	Facesheet separated from the foam core after 25 cycles (due to expansion of the foam with heat).
LH-5	Gr-Ep panel, EA 9394 adhesive, external Airex™ foam insulation, fiber-optics	50	No cracks. No disbonds.
LH-6	Gr-Ep panel, Crest 3170 adhesive, external Airex™ foam insulation, fiber-optics	50	No cracks. No disbonds.

† K3B - IM7/K3B

Compression Test

The compressive load capability of a tank wall concept under simulated structural and inertial loads will be tested using representative flat specimens in the cryogenic/high temperature compression test fixture shown in figure 14. This fixture and the flat specimens will also be used to induce a through-the-thickness temperature gradient in a compression specimen during a test.

In the compression test, a 0.60 m x 0.60 m (2 ft x 2 ft) specimen with cryogenic insulation will be subjected to a temperature load before a compressive load is introduced. Two temperature loading conditions will be attempted, a uniform temperature, and a constant temperature gradient through-the-thickness of the specimen. Three identical sandwich panels will be tested to failure. Each panel will experience one of three temperature load conditions: cryogenic temperature gradient (with a minimum temperature of 20 K, -423˚F and maximum temperature of 115K, -250˚F), room temperature, and a uniform elevated temperature (maximum temperature of 480 K, 400˚F).

The low-carbon, stainless steel (304 steel) compression load introduction fixtures shown in figure 14 were developed to introduce a uniform axial load across the top and bottom edge of the panel without requiring potting of the specimen's ends at cryogenic and high temperatures. These metallic fixtures were designed to control end displacement and to reduce bending effects from through-the-thickness temperature gradients, thus providing controlled boundary conditions at various temperatures. Conventional potting materials soften at temperatures above 450 K (350˚F) so their use was avoided. The metallic load introduction fixtures were designed to provide consistent and reproducible load transfer. Cryogenic and high temperature platens were developed to heat or cool the compression fixture to match the specimen's temperature. Ceramic insulation tiles will be used to reduce heat-loss through the platens and thermally isolate the compression fixture and platens from the load stand. Knife-edged supports (not shown in figure) composed of 304 stainless steel were also developed to impose simple-support boundary conditions on the vertical edges of the test specimen. The knife-edged supports have a temperature range from 80 K (-320˚F) to 480 K (400˚F). A Crest 3170 bellows seal was developed to contain the cryogenic fluid on the panel's cold side and resistive heater blankets will be used to heat the panel's faces.

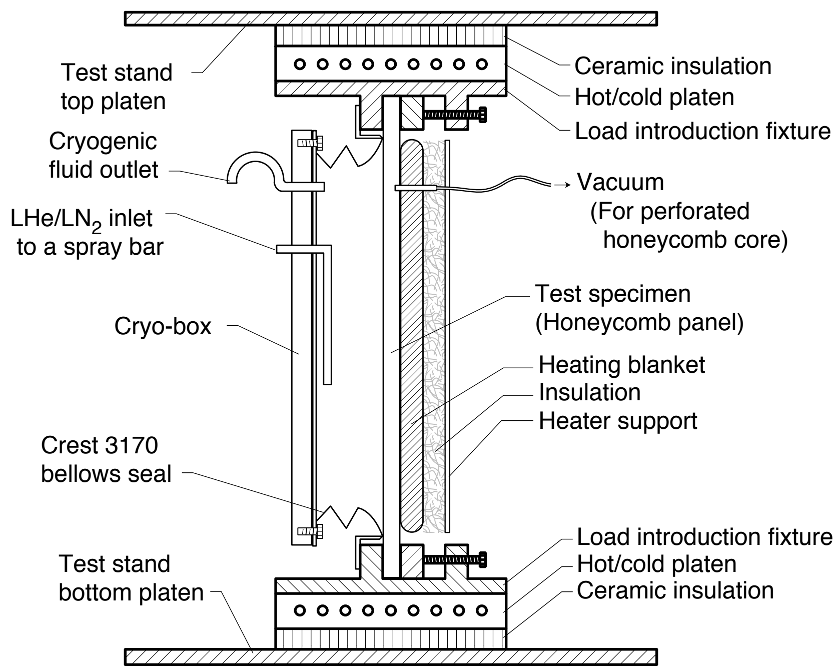

FIGURE 14. Schematic of the Cryogenic/Room/Elevated Temperature Compression Fixture.

Only the room-temperature panel test has been completed to date. The room-temperature honeycomb panel test consisted of co-cured IM7/K3B facesheets with a Ti honeycomb core (Gr-K3B/Ti/Gr-K3B). The K3B resin is a thermoplastic material that has a maximum operational temperature of 480 K (400˚F) and has non-autoclave joint fabrication potential. The upper and lower 0.06 m (2.5 in.) of the core were filled with a foaming adhesive during the curing process to facilitate load introduction from the fixture to the specimen and to prevent specimen "brooming" at the ends. However, the adhesive over-expanded in the core causing a discontinuity where the foam-filled region ended. Analysis predicted that the room-temperature panel would buckle in a panel buckling mode at a compressive load of 3110 kN (699 kips) or 5080 kN/m (29 kips/in.). Facesheet wrinkling was predicted to occur at a load of 707 kN (159 kips) or 1160 kN/m (6.63 kips/in.). The panel failed at a compressive load of only 540 kN (121 kips) or 880 kN/m (5.04 kips/in.) in the upper section of the panel adjacent to the aforementioned skin discontinuity. Failure in this region suggested that either the load was not properly introduced into the panel through the foam-filled honeycomb core region or that the panel was poorly fabricated near the edge of the foam-filled honeycomb core.

Subcomponent Test

A new test facility, the cryogenic pressure box, has been developed to validate full-scale tank subcomponents under realistic static and thermal/mechanical/pressure cyclical loading (Ambur, Sikora, Maguire, Winn 1996). Curved tank panel concepts can be tested at a relatively low cost compared to a full-scale or scaled tank tests at cryogenic temperatures. Analysis predicts that load distributions similar to those seen in a full-sized cylindrical tank can be produced in a 0.75 m x 1.0 m (2.5 ft x 3.5 ft) region in the center of the specimen. Check-out of the facility is in progress (February, 1998). The effects of cycling with mechanical loads, pressure loads, and thermal loads on full-scale assemblies of tank walls with cryogenic insulation, TPS, and IVHM can be determined with a full-scale subcomponent. Manufacturing and fabrication details can then be refined before fabrication of a full-scale tank, thus reducing the risk of premature failure due to cyclic thermal/mechanical loading.

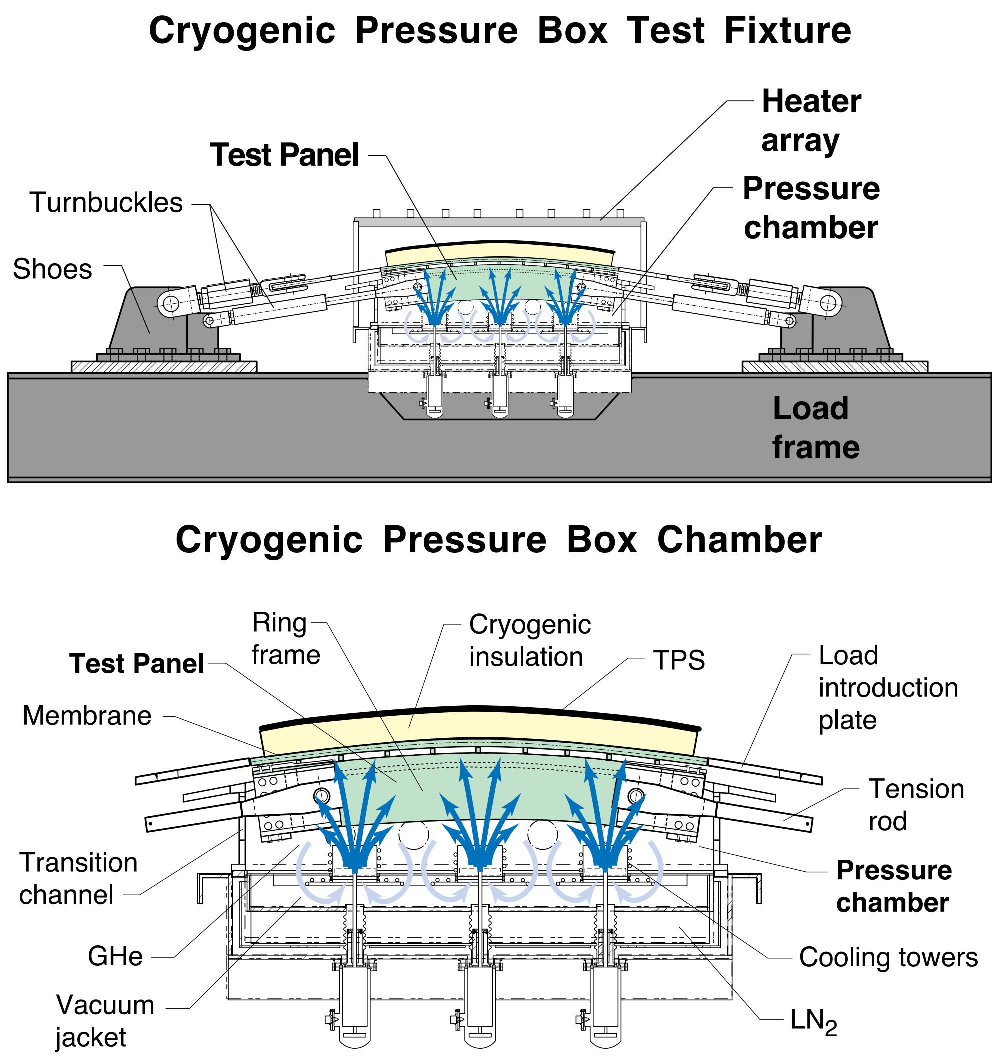

FIGURE 15. Schematic of the Cryogenic Pressure Box Test Fixture for Subcomponent Tests and the Cryogenic Pressure Chamber.

A schematic section view of the cryogenic pressure box fixture is shown in figure 15. In this subcomponent test, a 1.5 m x 1.8 m (5 ft x 6 ft) curved (radii of 2.0 m to 6.5 m, 80 in. to 260 in.) panel in figure 16 is loaded in biaxial tension by internal pressure and mechanical actuators. In addition, both cryogenic and elevated internal temperatures and a high external temperature can be applied. The biaxial tension load is introduced into the panel by internal pressure reacted through the load frame and by axial actuators. The maximum load applied by the axial actuators (not shown in figure 15) is 2000 kN (450 kips). Circumferential, or hoop, loads due to pressurization are induced by the reaction force from the load frame, through load introduction plates, into the test specimen. The vacuum jacketed pressure chamber can withstand internal pressures ranging from atmospheric to 372 kPa (54 psig) using GHe as the pressurization medium. The internal temperature of the chamber can be adjusted from 395 K (250˚F) to 20 K (-423˚F) with the aid of twelve copper heat exchange towers that are encircled by copper coils that contain either LHe, GHe or LN_2. The GHe is recirculated by fans through the heat exchange towers. Helium does not liquefy at temperatures above 15 K (-430˚F) and can be used to convectively cool the specimen and the pressure box chamber. The heat exchange towers also have resistive heaters at their bases, enabling internal heating of the chamber and the internal surface of the panel to a maximum temperature of 395 K (250˚F). A quartz-lamp heater array is used to heat the external surface of the specimen to a maximum temperature of 810 K (1000˚F). The heater array is flat and has eight symmetric zones that can be individually controlled to evenly heat specimens of various curvatures.

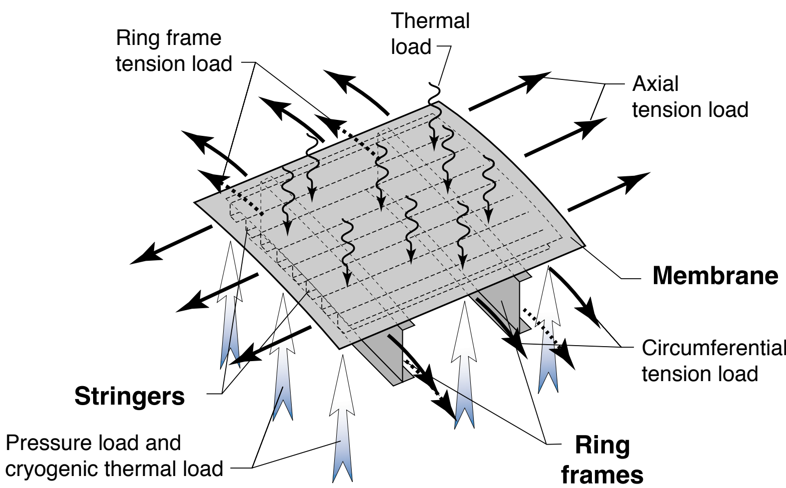

FIGURE 16. Thermal and Mechanical Loads Applied to a Representative Specimen in the Cryogenic Pressure Box Test Fixture.

A representative X-33 LH_2 tank specimen is scheduled to be tested in the spring of 1998 in the cryogenic pressure box for Lockheed-Martin Michoud Space Systems. The specimen will consist of Gr-Ep facesheets with a Korex™ honeycomb core and will also have representative hoop and bulkhead joints. Fiber optic, IVHM sensors will monitor the temperatures and strains of the specimen. Load and temperature profiles similar to those utilized in the uniaxial tension test, shown in figure 13, will be used. The effects of pressurization, cryogenic temperatures, and elevated temperatures on the specimen will be monitored to verify the integrity of the fabrication process and performance of a full-scale tank system.

SUMMARY

A systematic approach was used in the research for the design of integrated cryogenic tank systems for an RLV. This approach began with thermal and structural analytical studies followed by testing of specimens ranging from elements to subcomponents at the NASA Langley Research Center.

The results of the analytical studies identified honeycomb sandwich tank with mechanically attached metallic TPS as an attractive approach for a reusable LH_2 tank system for an RLV. The two most attractive honeycomb sandwich concepts were found to be (Gr-BMI/HRP/Gr-BMI) and (Ti/Ti/Ti).

Element tests were used to evaluate bonding and fabrication methods as well as the evacuation process for sandwich tank structures. Adhesives such as Crest 3170 and HT 435 were identified as attractive for cryogenic tank construction by the flatwise tension tests. The evacuated honeycomb sandwich (ravioli) tests demonstrated that sealed sandwich concepts may be problematic, that evacuation of a sandwich is difficult, and that active evacuation may be a solution to obtain a reliable sandwich tank concept.

The panel and subcomponent tests developed or in various stages of development, investigate structural strength and durability, the reliability of the fabrication process scale-up, thermal properties, and bond line integrity of cryogenic tank designs. The uniaxial tension tests provided data for the X-33 Program in support of certifying SS-1171 for the LOX tank and a new cryogenic foam insulation, Airex™, for the LH_2 tanks. The compression fixture will enable the testing of specimens at various temperatures or with through-the-thickness temperature gradients. Full-scale tank sections with cryogenic insulation and TPS will be tested at cryogenic and elevated temperatures with a pressure load and under biaxial tension in the cryogenic pressure box fixture at a fraction of the cost to test full or scaled tanks.

The unique analytical tools and facilities developed at the NASA Langley Research Center during Phase I and Phase II of the X-33/RLV Program enable the study and testing of various cryogenic tank concepts at operational thermal loads, mechanical loads, and pressure loads. The results obtained from these analytical and experimental cryogenic tank studies will provide vital information required to develop full-scale, reusable, and integrated cryogenic tanks for future reusable launch vehicles.

Acknowledgments

The research conducted at LaRC could not have been accomplished without the efforts of the members of the cryogenic tank team in the Thermal Structures Branch (TSB). The cryogenic tank team was supported by systems specialists Mr. Joseph Sikora and Mr. Vincent LeBoffe, designer Mr. Kermit Jensen, structural analysts Mr. Carl Martin and Mr. Jeff Cerro and all of the technical staff in the TSB laboratory but especially electrician Mr. Paul McClung for developing the control algorithms for the uniaxial tension tests. Optimization analyses was performed by Mr. Satchi Venkataraman and Dr. Raphael Haftka at the University of Florida. The cryogenic pressure box development was conducted with Dr. Damodar Ambur, Dr. David Glass, Mr. Marshall Rouse, Mr. Henry Wright, Mr. James Mayhew, and Mr. Carlos Perez. Many of the original cryogenic tank team's concepts, analytical studies, and tests were initiated by Dr. Charles Camarda.

References

Freeman, Jr., D. C., Stanley, D. O., Camarda, C. J., Lepsch, R. A., Cook, S. A. (1994) "Single-Stage-To-Orbit-A Step Closer," Presented at the 45th Congress of the International Astronautical Federation (IAF), October 1994, IAF 94-V3.534.

NASA (1993) "Access to Space Study Final Report," NASA Headquarters, Washington DC, July 1993.

Baumgartner, R. I. (1997) "Venturestar™ Single Stage to Orbit Reusable Launch Vehicle Program Review," Presented at the Space Technologies and Application International Forum, Albuquerque, NM, January 1997, Vol. 3: 1033-1039.

Cook, S. (1996) "The X-33 Advanced Technology Demonstrator," Presented at the American Institute of Aeronautics and Astronautics (AIAA) Dynamics Specialists Conference, April 1996, AIAA-96-1195.

Melvin, L., Childers, B., Rogowski, R., Prosser, W., Moore, J., Froggatt, M., Allison S., Wu, M. C., Bly, J., Aude, C., Bouvier, C., Zisk, E., Enright, E., Cassadaban, Z., Reightler, R., Sirkis, J., Tang, I., Peng, T., Wegreich, R., Garbos, R., Mouyos, W., Aibel, D., Bodan, P. (1997) "Integrated Vehicle Health Monitoring (IVHM) for Aerospace Vehicles," Presented at the International Workshop on Structural Health Monitoring, Structural Health Monitoring: Current Status and Perspectives, Edited by Fu-Kuo Chang, Stanford, CA, September 1997, pp. 705-714.

Anonymous I (1995) "Prototype Tank Drawings and Analysis," Reusable Composite Hydrogen Tank System TA 1 Payment Milestone 14, Part 2 of 5, Cooperative Agreement NCC8-39, Rockwell International, September 1995, SSD95D0388.

Anonymous II (1995) "Test Report of Element/Subcomponent Testing," Reusable Composite Hydrogen Tank System TA 1 Payment Milestone 16, Part 1 of 2, Cooperative Agreement NCC8-39, Rockwell International, November 1995, SSD95D0507.

Myers, D. E. Martin, C. J., Blosser, M. L. (1997) "Parametric Weight Comparison of Advanced Metallic, Ceramic Tile, and Ceramic Blanket Thermal Protection Systems (TPS)," NASA Technical Memorandum L-17651, August 1997.

Bushnell, D. (1977) "BOSOR4: Program for Stress and Vibration of Shells of Revolution," Structural Mechanics Software Series, Edited by N. Perrone and W. Pilkey, University Press of Virginia, Charlottesville, VA, Vol. 1: 11-143.

Glass, D. E. (1997) "Bonding and Sealing Evaluations for Cryogenic Tank," NASA Contractor Report 201734, August 1997.

McAuliffe, P. S., Davis, R. C., Taylor, A. H. (1986) "Development of Reusable, Flight-Weight Cryogenic Foam Insulation System," Presented at the American Institute of Aeronautics and Astronautics (AIAA) Space Systems Technology Conference, June 1986, AIAA-1189-CP.

Ambur, D. R., Sikora, J., Maguire, J. F. Winn, P. M. (1196) "Development of Pressure Box to Evaluate Reusable Launch-Vehicle Cryogenic Tank Panels," Presented at the American Institute of Aeronautics and Astronautics (AIAA) 37th AIAA/ASME/ASCE/AHS/ASC Structures, Structural Dynamics, and Materials Conference, April 1996, AIAA-96-1640.

Nomenclature

304 steel:	Stainless Steel
AETB:	Alumina Enhanced Thermal Barrier
Al:	Aluminum 2219-T87
Al-Li:	Aluminum-2195
ALS:	Advanced Launch System
ELI:	Extra Low Interstitial
Gr-BMI:	IM7/5260 Graphite-Bismaleimide
Gr-Ep:	IM7/977-2 Graphite-Epoxy
GHe:	Gaseous Helium
He:	Helium
HRP:	Hexcel™ glass Reinforced Phenolic
IVHM:	Integrated Vehicle Health Monitoring
K3B:	IM7/K3B
LaRC:	Langley Research Center
LH_2:	Liquid Hydrogen
LHe:	Liquid Helium
LOX:	Liquid Oxygen
NASA:	National Aeronautics and Space Administration
Nx:	Axial Load
RLV:	Reusable Launch Vehicle
SA/HC:	Superalloy/Honeycomb
SOFI:	SS-1171 Spray On Foam
SSTO:	Single-Stage-To-Orbit
TABI:	Tailorable Advanced Blanket Insulation
Ti:	Titanium
TPS:	Thermal Protection System
TSB:	Thermal Structures Branch
VAB:	Vehicle Analysis Branch